



Fischer, Andreas

Angular-Dependent Radius Measurements at Rotating Objects Using Underdetermined Sensor Systems

Journal Article as: peer-reviewed accepted version (Postprint)

DOI of this document\* (secondary publication): <https://doi.org/10.26092/elib/3307>

Publication date of this document: 13/09/2024

\* for better findability or for reliable citation

Recommended Citation (primary publication/Version of Record) incl. DOI:

A. Fischer, "Angular-Dependent Radius Measurements at Rotating Objects Using Underdetermined Sensor Systems," in IEEE Transactions on Instrumentation and Measurement, vol. 67, no. 2, pp. 425-430, Feb. 2018, doi: 10.1109/TIM.2017.2777558

Please note that the version of this document may differ from the final published version (Version of Record/primary publication) in terms of copy-editing, pagination, publication date and DOI. Please cite the version that you actually used. Before citing, you are also advised to check the publisher's website for any subsequent corrections or retractions (see also <https://retractionwatch.com/>).

© 2018 IEEE. Personal use of this material is permitted. Permission from IEEE must be obtained for all other uses, in any current or future media, including reprinting/republishing this material for advertising or promotional purposes, creating new collective works, for resale or redistribution to servers or lists, or reuse of any copyrighted component of this work in other works.

This document is made available with all rights reserved.

Take down policy

If you believe that this document or any material on this site infringes copyright, please contact [publizieren@suub.uni-bremen.de](mailto:publizieren@suub.uni-bremen.de) with full details and we will remove access to the material.

# Angular-Dependent Radius Measurements at Rotating Objects Using Underdetermined Sensor Systems

Andreas Fischer, *Member, IEEE*

**Abstract**—Precise and contactless shape measurements of rotating objects is important, e.g., for monitoring and controlling the manufacturing quality in lathes. For this purpose, multisensor and single-sensor approaches based on optical distance and surface velocity measurements are state-of-the-art techniques. Two- and single-sensor systems are particularly promising to measure the angular-dependent radius of the cross section of the rotating object in a scanning regime with minimal optical access. Since a comparison between the different sensor systems is missing, the potential of these underdetermined sensor systems is unclear. In addition, displacements of the rotational axis and sensor misalignments are suspected to be crucial error sources, but the error is unknown. For this reason, an error analysis is performed regarding the resulting systematic error and the random error for the two- and single-sensor systems. As a result, the different sensor systems have an equal cross-sensitivity with respect to lateral displacements of the rotational axis from the sensor axes, but the two-sensor approach has the lowest sensitivity regarding sensor misalignments. For the studied measurement conditions, the systematic error dominates the sensor noise for the two-sensor system and the single-sensor system with combined distance and velocity measurement at an object mean radius  $>6$  mm. The smallest total measurement uncertainty is obtained with the two-sensor system. Finally, the relevance of systematic error depends on the utilization, i.e., for instance on the absolute rotor radius, the stability of the rotor axis, the sensor position, the accuracy of the sensor alignment, and the uncertainty of the distance and/or velocity measurements.

**Index Terms**—Inverse problem, measurement uncertainty, optical radius measurement, shape measurement, systematic and random errors.

## I. INTRODUCTION

**O**PTICAL *in situ* shape measurements of rotating objects with micrometer and submicrometer precision are required, e.g., for monitoring the machining process in lathes [1], [2] or the deformation of rotors with new materials such as composite materials in rotor test rigs [3]. The main challenge is to measure the 2-D shape, i.e., the cross section of the rotating object perpendicular to the rotational axis, because 3-D shape measurements can then be achieved by scanning along the height axis. In order to cope with the

large object's diameter, which is usually more than five orders of magnitude larger than the desired resolution [4], [5], and due to limited space and limited optical access, systems with multiple distance sensors are applied. A multisensor system with  $N \in \mathbb{N}$  equally spaced sensors along a virtual circle around the measurement object is depicted in Fig. 1(a). A huge variety of applicable distance sensors exist such as intensity-based sensors, triangulation sensors, time-of-flight sensors, confocal sensors, and interferometric sensors [6], [7]. In addition, interferometric laser Doppler distance sensors were developed, which are based on the speckle effect and are well-suited for optically rough surfaces and high surface velocities or high rotor speeds, respectively [8]–[10]. Further measurement principles exist in particular for the diameter measurement of round objects, which evaluate the optical diffraction pattern behind the measurement object [11], [12].

Multisensor systems can measure arbitrary shapes by scanning the angular-dependent radius of the object during the rotation [4]. However, this circumferential scanning requires a no whirling assumption, i.e., the unknown movement of the rotational axis is considered to be negligible. If whirling occurs the measurement system is undetermined and thus the measurement uncertainty increases [3]. The minimal configuration of a multisensor system is a two-sensor system where the sensors are located oppositely. For this configuration, only a displacement of the rotational axis perpendicular to the sensor axes leads to a respective measurement error.

If the shape is not arbitrary, but can be determined from  $N$  points in space, it is possible to determine the object shape without scanning by applying a multisensor system with  $N$  sensors. For instance, a circular shape requires at least three sensors [13] and an elliptical shape requires at least five sensors [3]. The subsequent investigation focuses on the scanning techniques. However, if the minimal necessary number of sensors is not feasible (for instance, due to the limited access) or an unwanted setting, the no whirling assumption is applicable or the unpredictable movement of the rotational axis will also lead to a measurement error.

A single-sensor system with a single distance sensor minimizes the number of optical accesses, but lateral and axial displacements of the rotational axis with respect to the sensor axis cause errors. Moreover, it is crucial to know the initial axial axis position precisely. In order to overcome this limitation, it is beneficial to derive the object radius from the known rotational frequency and a measurement of the tangential surface velocity, because the velocity is not affected by axial

Manuscript received July 14, 2017; revised September 08, 2017; accepted September 27, 2017. Date of publication December 13, 2017; date of current version January 4, 2018. The Associate Editor coordinating the review process was Dr. George Xiao.

The author is with the Bremen Institute for Metrology, Automation, and Quality Science, University of Bremen, 28359 Bremen, Germany (e-mail: andreas.fischer@bimaq.de).

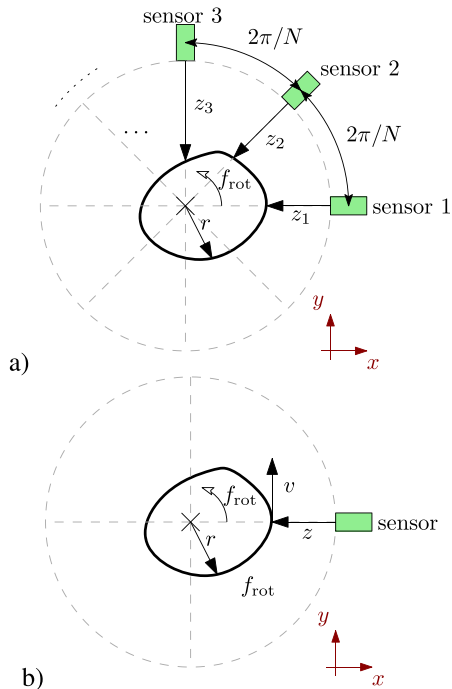


Fig. 1. Shape measurement of rotating objects using (a)  $N$  distance sensors (multisensor system) and (b) single sensor that measures distance and surface velocity simultaneously (single-sensor system). The rotational frequency is  $f_{\text{rot}}$ . The  $x$  marks the rotational axis.

displacements of the rotational axis [14]. Note that this single-sensor system is still underdetermined under general whirling conditions with lateral axis displacements.

A more precise single-sensor system was developed [15] and applied in lathes [2] where the sensor-surface distance and the tangential surface velocity are measured simultaneously [see Fig. 1(b)]. Using the known rotational frequency, the mean value of the velocity measured over one revolution allows to determine the mean radius of the object, and the radial deviations from a circular shape with such a mean radius follow from the distance measurements. Hence, the initial axial position of the rotational axis is not required. However, the effect of rotor axis displacements remains to be investigated.

For the shape measurement with underdetermined multi-sensor and single-sensor systems, the whirling motion or the displacement of the rotational axis results in a measurement error. However, the error magnitude is an open question. Even more important, a comparison between the respective benefits and drawbacks of the different measurement approaches is missing. The same is true regarding sensor misalignments, because the imperfect alignment of multiple sensors is suspected to cause a significant contribution to the measurement uncertainty.

Due to these reasons, a fundamental model-based comparison has been undertaken between the two-sensor approach based on two distance sensors, the single-sensor approach based on a velocity sensor, and the single-sensor approach based on a combined velocity and distance sensor. First, the different measurement principles and the respective model equations to determine the angular-dependent radius of the rotating object are explained in Section II. The different

measurement approaches are then compared regarding the random errors due to the sensor noise in Section III. Subsequently in Section IV, the systematic error due to displacements of the rotational axis and due to sensor misalignments are calculated and discussed by means of a simulation. The article closes by summarizing the key findings in Section V.

## II. MEASUREMENT PRINCIPLES

### A. Two-Sensor System

The case of two distance sensors is considered similar to the sketch in Fig. 1(a), where  $N = 2$ . The angular distance between both sensors amounts to  $\pi$ , i.e., the two sensors are aligned at opposite sides. In this particular case, the sensor axes are antiparallel and intersect the rotational axis.

The radius  $r$  of the object at the observed angle is obtained from the two measured distances  $z_1, z_2$  and the diameter  $D$  of the calibration object (for which the distance signals were set to zero)

$$r = \frac{1}{2}(D - (z_1 + z_2)). \quad (1)$$

The angular-dependent radius of the object is determined from repeated measurements during the rotation with known angles.

An axial displacement of the rotational axis does not disturb the measurement, because the evaluated sum  $z_1 + z_2$  of the sensor signals is not affected. However, a cross-sensitivity with respect to the lateral displacement of the rotational axis exists.

### B. Single-Sensor System ( $v$ )

The case of a single sensor corresponds to the sketch in Fig. 1(b), but only the lateral velocity  $v$  of the object surface is measured here.

Assuming that the sensor axis intersects the rotational axis, the radius of the rotating object is measured by calculating

$$r = \frac{v}{2\pi f_{\text{rot}}} \quad (2)$$

with  $f_{\text{rot}}$  as known rotational frequency. As for the two-sensor approach, the angular-dependent radius of the object results from the repeated measurement.

An axial displacement of the rotational axis has no effect on the velocity and thus no effect on the radius measurement. A lateral displacement of the rotational axis disturbs the measurement.

### C. Single-Sensor System ( $v, z$ )

The single-sensor approach with a combined velocity and distance measurement is depicted in Fig. 1(b). According to the underlying measurement principle, the object radius  $r$  is divided into the object mean radius  $R$  and the radial deviation  $r_{\Delta} = r - R$  from the mean radius

$$r = R + r_{\Delta}. \quad (3a)$$

According to (2), the object mean radius is obtained from the mean velocity  $V$  measured over one revolution by the relation

$$R = \frac{V}{2\pi f_{\text{rot}}}. \quad (3b)$$

The radial deviation results from the distance measurement  $z$  by calculating

$$r_{\Delta} = -(z - Z) \quad (3c)$$

where  $Z$  is the mean distance of the measured object over one revolution.

The measurement principle is based on the assumption that the movement of the rotational axis along the sensor axis is negligible with respect to the distance measurement uncertainty. A constant axial displacement of the rotational axis has no effect on the measurement result, whereas lateral axis displacements always have.

### III. RANDOM ERROR

The different measurement approaches are compared with respect to the measurement uncertainty resulting from random sensor errors. For this purpose, an error propagation calculation is applied to the model equations (1)–(3) derived in Section II. The calibration uncertainty is assumed negligible in all discussed cases. The standard uncertainty of the distance and the velocity measurement is denoted by  $u(z)$  and  $u(v)$ , respectively. In order to complement the findings by quantitative results, the typical values  $u(z) = 2 \mu\text{m}$  [16] and  $u(v) = 0.2\%$  [8] are applied below. Using a laser Doppler velocimeter as velocity sensor, the relative velocity uncertainty is usually constant [17].

For the two-sensor system (1), the standard deviation of the angular-dependent radius that results from an error propagation calculation amounts to

$$u(r) = \frac{1}{\sqrt{2}}u(z) \quad (4)$$

because the distance signals of both sensors are uncorrelated. Hence, the magnitude of the radius uncertainty is almost equal to the uncertainty of the distance sensors. This means a typical radius uncertainty in the order of  $2 \mu\text{m}$ .

The model of the single-sensor approach based on velocity measurements (2), leads to

$$u(r) = \frac{1}{2\pi|f_{\text{rot}}|}u(v) = r \frac{u(v)}{|v|}. \quad (5)$$

As a result, the radius uncertainty is directly proportional to the object radius. Consequently, the single-sensor approach is superior to the two-sensor system for objects with a small radius, namely, if  $r < u(z)(1/\sqrt{2}/u(v)/|v|)$ . For the typical uncertainty values, the limiting radius size reads  $0.5 \text{ mm}$ . Since the object radius is in general larger, the single-sensor approach suffers from a comparatively high uncertainty.

For the single-sensor approach with the combined velocity and distance measurement, an error propagation applied to the model (3) gives the radius standard deviation

$$\begin{aligned} u(r) &= \sqrt{\left(r \frac{u(v)}{|v|}\right)^2 \cdot \frac{1}{M} + u(z)^2 \cdot \left(1 + \frac{1}{M}\right)^2 + \frac{u(z)^2}{M^2} \cdot (M-1)} \\ &\approx \sqrt{\left(r \frac{u(v)}{|v|}\right)^2 \cdot \frac{1}{M} + u(z)^2}, \quad M \gg 1. \end{aligned} \quad (6)$$

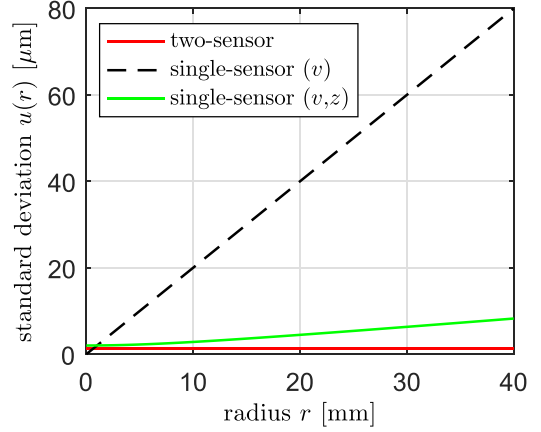


Fig. 2. Standard deviation of the angular-dependent object radius  $r$  with respect to the object radius for the considered measurement approaches. The results follow from an uncertainty analysis according to the international guide to the expression of uncertainty and using the parameters  $u(z) = 1 \mu\text{m}$ ,  $(u(v)/|v|) = 0.1\%$ ,  $M = 100$ .

Note that a sensor configuration is considered where no correlation between the distance and the velocity measurement values occurs. The symbol  $M$  denotes the number of acquired samples of the sensor output signals while the object is rotating. Here  $M$  velocity values and  $M$  distance values are used for the radius measurement. For sufficiently large  $M$ , the influence of the velocity uncertainty is smaller than the influence of the distance uncertainty. Since the remaining contribution from the distance uncertainty is typically smaller than the uncertainty for the single-sensor approach without additional distance measurement ( $u(z) < r(u(v)/|v|)$ ), the combined distance and velocity measurement is identified as the better suited method based on the presented comparison for random error sources.

When comparing with the two-sensor approach, however, the extended single-sensor approach turns out to be always less precise. The characteristic object radius for which the uncertainty becomes, for instance,  $\sqrt{2}u(z)$  (i.e., a factor of  $\sqrt{2}$  larger than using a single distance sensor) is  $u(z)(\sqrt{M}/u(v)/|v|)$ . Assuming  $M = 100$ , this characteristic radius amounts to  $10 \text{ mm}$ .

In order to summarize the behavior of the three measurement settings, the radius standard deviation is shown in Fig. 2 over the object radius. Note that the measurement uncertainty due to random errors can be reduced by evaluating multiple revolutions.

### IV. SYSTEMATIC ERROR

All measurement approaches have a cross-sensitivity with respect to a lateral displacement of the rotational axis. The same holds for sensor misalignments. The underdetermined two- and single-sensor approaches require the rotational axis to intersect the sensor axis. The condition is not fulfilled either if the rotational axis shows a displacement or if the sensor alignment is not as intended. These cases are discussed in Sections IV-A and IV-B, respectively.

In order to quantify the resulting measurement errors, a MATLAB simulation based on the model equations in Section II and the geometry of the measurement arrangement

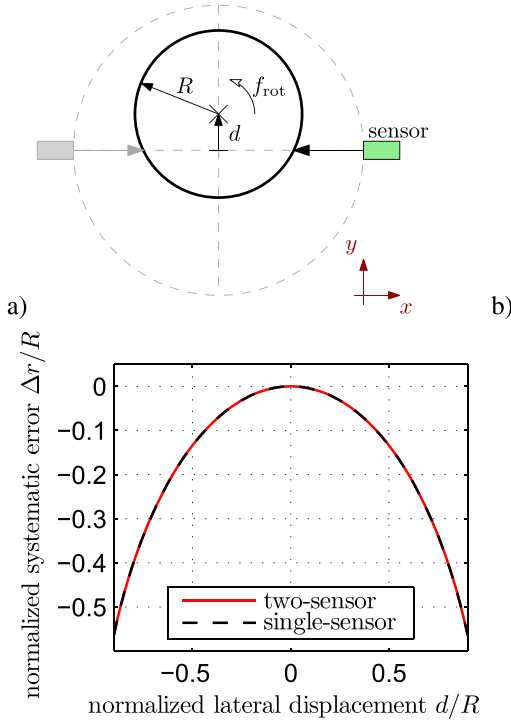


Fig. 3. (a) Lateral displacement  $d$  of the rotational axis and (b) resulting systematic error  $\Delta r$  normalized by the radius  $R$  of the circular object as a function of the normalized displacement  $d/R$ . The error applies for the two-sensor system as well as for both single-sensor systems.

is performed. For simplification, the object shape is assumed to be circular with the radius  $r = R$  and the displacements or misalignments are assumed to be constant during one rotor revolution. As a result,  $z - Z = 0$  in (3) and, thus, both single-sensor approaches give equal results. For this reason, it is only distinguished between the two- and the single-sensor approach in this section.

#### A. Displacement of the Rotational Axis

The case of a lateral displacement  $d$  of the rotational axis and the resulting systematic error are shown in Fig. 3. Surprisingly, the systematic error is the same for the two- and single-sensor approaches. Considering, for instance, a relative displacement of  $(d/R) = 5\%$ , the systematic error amounts to  $\Delta r = 0.1\% \cdot R$ , which means already  $\Delta r = 2 \mu\text{m}$  for  $R = 2 \text{ mm}$ . Since the object radius is typically larger, such lateral displacements are in general not negligible compared to the sensor uncertainty. However, this conclusion has to be drawn separately for each application with the respective displacement  $d$ .

#### B. Sensor Misalignment

In general, an axial sensor misalignment leads to a measurement error for the two-sensor system. According to an error propagation calculation applied to (1), the resulting error is  $\Delta r = -(1/2)(\Delta z_1 + \Delta z_2)$ . The error only vanishes for  $\Delta z_1 = -\Delta z_2$ . On the contrary, no error results for the single-sensor systems.

Lateral sensor misalignments lead to a systematic error for all measurement approaches. Since the sensor displacement

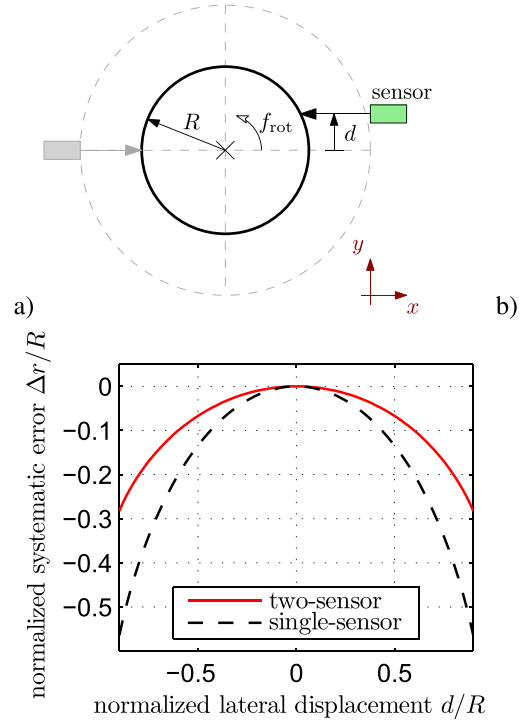


Fig. 4. (a) Lateral displacement  $d$  of one sensor and (b) resulting systematic error  $\Delta r$  normalized by the radius  $R$  of the circular object as a function of the normalized displacement  $d/R$ .

can be interpreted as a respective opposite displacement of the rotational axis, the error discussed in Section IV-A results. This statement holds for both single-sensor settings as well as for the two-sensor system when the displacement of the two sensors is equal [see Fig. 3(a)]. However, for the two-sensor system, the displacement of each sensor can be different. As an example, the scenario of one misaligned sensor is presented in Fig. 4. The absolute value of the resulting error for the two-sensor approach is lower than for two equally misaligned sensors (see Fig. 3), and lower than for an equally misaligned sensor using the single-sensor approaches.

The sensor misalignment can also mean a tilt of the sensor axis [see Fig. 5(a)]. Note that the resulting error depends on the angular displacement  $\alpha$  as well as the radial position  $L$  of the sensors (or the relative object radius  $R/L$ , respectively). As an example, the error is shown in Fig. 5(b) with respect to the angular displacement for the measurement arrangement  $L = 2 R$ . The two-sensor approach has a lower cross-sensitivity than the single-sensor approaches. For a typical angle  $\alpha = 2^\circ$ , e.g., the error amounts to  $-0.06\% \cdot R$  and  $-0.25\% \cdot R$ , respectively. Hence, the absolute value of the error amounts  $2 \mu\text{m}$  for  $R = 3.3$  and  $0.8 \text{ mm}$ , respectively. Since the objects are usually larger, the angular displacement of a sensor can mean a serious contribution to the shape measurement uncertainty.

#### C. Combined Uncertainty

In order to demonstrate the significance of the systematic error or the random error, respectively, the combined uncertainty is shown in Fig. 6 over the mean object radius together with the random error from Fig. 2. As systematic error, a

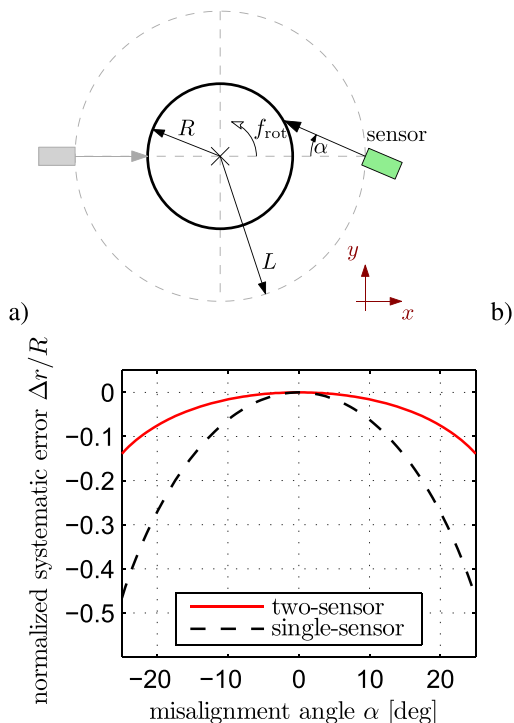


Fig. 5. (a) Angular misalignment  $\alpha$  of one sensor and (b) resulting systematic error  $\Delta r$  normalized by the radius  $R$  of the circular object. Note that  $L = 2R$  is applied here as an example.

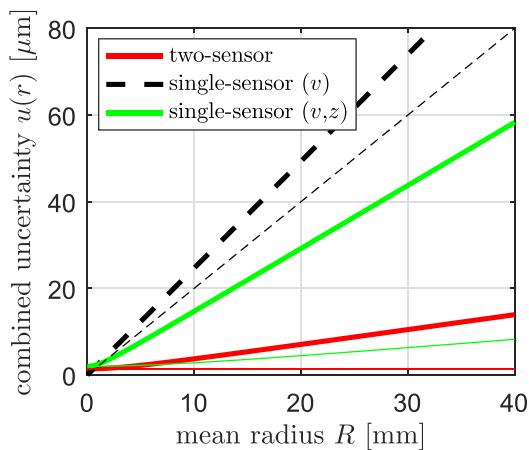


Fig. 6. Combined standard uncertainty of the object radius  $r$  with respect to the object mean radius  $R$  for a relative unknown systematic error of  $\pm 0.06\%$  (two-sensor system) and  $\pm 0.25\%$  (single-sensor systems), respectively, due to an angular misalignment of the sensor located at  $L = 2R$  (see Fig. 5), and for the random error shown in Fig. 2. The combined standard uncertainty (thick curves) is compared with the contribution from the random error (thin curves).

relative error of  $\pm 0.06\%$  is considered for the two-sensor system, and a relative error of  $\pm 0.25\%$  is taken into account for both single-sensor settings. These errors correspond to an angular sensor misalignment of  $\pm 2^\circ$  for a sensor position at  $L = 2R$  [see Section IV-B, Fig. 5(a)].

As a result for the single-sensor setting with the velocity evaluation, the contribution from the random error to the measurement uncertainty is larger than the contribution from the systematic error in the shown range of the mean object radius. In contrast to this behavior, the random error is negligibly small for the single-sensor setting with velocity

and distance measurement as well as for the two-sensor setting considering large mean object radiuses  $R > 2$  mm and  $R > 6$  mm, respectively. Hence, the systematic error typically dominates the total measurement uncertainty at large measurement objects. Furthermore, the lowest total uncertainty is obtained with the two-sensor approach.

## V. CONCLUSION

The investigated single-sensor settings offer the lowest requirements with respect to the optical access and the number of sensors to be aligned. On the other hand, the measurement uncertainty of the angular-dependent object radius resulting from the typical uncertainties of the sensor signals is minimal for the two-sensor system. In particular, the radius measurement uncertainty is independent of the object radius for a two-sensor system, but is increasing with the object radius for both single-sensor systems. Furthermore, the single-sensor setting with the combined measurement of the lateral surface velocity and the surface distance was shown to be superior to the single-sensor setting with the sole measurement of the surface velocity.

Sensor misalignments and displacements of the rotational axis can occur, which contribute to the radius measurements uncertainty of underdetermined measurement systems. Such underdetermined systems are, e.g., the two-sensor system based on distance measurements, the single-sensor system based on velocity measurements, and the single-sensor system based on combined velocity and distance measurements. While the two-sensor system is affected by axial and lateral displacements of the rotational axis, both single-sensor systems are only disturbed by lateral displacements (as long as the axial displacement during one rotor revolution is negligible). The cross-sensitivity regarding a lateral displacement of the rotational axis is equal for all three sensor systems. Regarding sensor misalignment issues, however, the two-sensor system is superior to the single-sensor systems. For the single-sensor settings, only a single sensor has to be aligned, but the alignment requirements are higher than for the two-sensor setting.

The misalignment of the sensors and the displacement of the rotational axis cause systematic errors, which can dominate the overall radius measurement uncertainty at measurement objects with a large mean radius. Using the described error analysis, the influence of random and systematic errors can now be determined for each application. Vice versa, the experiment can now be designed to achieve the desired accuracy by formulating (and then realizing) the necessary requirements with respect to the rotor axis stability, the alignment of the sensors and the uncertainty of the sensors. Furthermore, future studies should focus on multisensor systems with more than two sensors.

## REFERENCES

- [1] K. Vacharanukul and S. Mekid, "In-process dimensional inspection sensors," *Measurement*, vol. 38, no. 3, pp. 204–218, 2005.
- [2] R. Kuschmierz *et al.*, "Optical, *in situ*, three-dimensional, absolute shape measurements in CNC metal working lathes," *Adv. Manuf. Technol.*, vol. 84, no. 9, pp. 2739–2749, 2016.

- [3] K. Philipp *et al.*, “Multi-sensor system for *in situ* shape monitoring and damage identification of high-speed composite rotors,” *Mech. Syst. Signal Process.*, vols. 76–77, pp. 187–200, Aug. 2016.
- [4] S. Mekid and K. Vacharanukul, “In-process out-of-roundness measurement probe for turned workpieces,” *Measurement*, vol. 44, pp. 762–766, May 2011.
- [5] R. Kuschmierz *et al.*, “In-process, non-destructive, dynamic testing of high-speed polymer composite rotors,” *Mech. Syst. Signal Process.*, vols. 54–55, pp. 325–335, Mar. 2015.
- [6] G. Berkovic and E. Shafir, “Optical methods for distance and displacement measurements,” *Adv. Opt. Photon.*, vol. 4, no. 4, pp. 441–471, 2012.
- [7] P. Pavliček and G. Häusler, “Methods for optical shape measurement and their measurement uncertainty,” *Int. J. Optomechatron.*, vol. 8, no. 4, pp. 292–303, 2014.
- [8] T. Pfister, L. Büttner, and J. Czarske, “Laser Doppler profile sensor with sub-micrometre position resolution for velocity and absolute radius measurements of rotating objects,” *Meas. Sci. Technol.*, vol. 16, no. 3, pp. 627–641, 2005.
- [9] F. Dreier, P. Günther, T. Pfister, J. W. Czarske, and A. Fischer, “Interferometric sensor system for blade vibration measurements in turbomachine applications,” *IEEE Trans. Instrum. Meas.*, vol. 62, no. 8, pp. 2297–2302, Aug. 2013.
- [10] R. Kuschmierz, J. Czarske, and A. Fischer, “Multiple wavelength interferometry for distance measurements of moving objects with nanometer uncertainty,” *Meas. Sci. Technol.*, vol. 25, no. 8, pp. 085202-1–1085202-8, 2014.
- [11] J. Li, O. Sasaki, and T. Suzuki, “Measurement of diameter of metal cylinders using a sinusoidally vibrating interference pattern,” *Opt. Commun.*, vol. 260, no. 2, pp. 398–402, 2006.
- [12] Y. A. Chursin and E. M. Fedorov, “Methods of resolution enhancement of laser diameter measuring instruments,” *Opt. Laser Technol.*, vol. 67, pp. 86–92, Apr. 2015.
- [13] P. Günther, F. Dreier, T. Pfister, J. Czarske, T. Haupt, and W. Hufenbach, “Measurement of radial expansion and tumbling motion of a high-speed rotor using an optical sensor system,” *Mech. Syst. Signal Process.*, vol. 25, no. 1, pp. 319–330, 2011.
- [14] K. Vacharanukul and S. Mekid, “New real-time non-contact probe using Gaussian convolution smooth technique for in-process inspection,” *Sens. Actuators A, Phys.*, vol. 141, no. 1, pp. 20–28, 2008.
- [15] P. Günther, R. Kuschmierz, T. Pfister, and J. W. Czarske, “Displacement, distance, and shape measurements of fast-rotating rough objects by two mutually tilted interference fringe systems,” *J. Opt. Soc. Amer. A, Opt. Image Sci.*, vol. 30, no. 5, pp. 825–830, 2013.
- [16] R. G. Dorsch, G. Häusler, and J. M. Herrmann, “Laser triangulation: Fundamental uncertainty in distance measurement,” *Appl. Opt.*, vol. 33, no. 7, pp. 1306–1314, 1994.
- [17] B. E. Truax, F. C. Demarest, and G. E. Sommargren, “Laser Doppler velocimeter for velocity and length measurements of moving surfaces,” *Appl. Opt.*, vol. 23, no. 1, pp. 67–73, 1984.



**Andreas Fischer** (M'16) received the Ph.D. degree and the *venia legendi* degree in electrical engineering from Technische Universität Dresden, Dresden, Germany, in 2009 and 2013, respectively.

From 2009 to 2016, he was the head of the group of measurement system techniques at the Laboratory for Measurement and Testing Techniques of the Technische Universität Dresden. Since 2016, he has been a Full Professor with the University of Bremen, Bremen, Germany, where he is the Director of the Bremen Institute for Metrology, Automation, and

Quality Science. His current research interests include the identification, characterization, and application of measurement limits as well as the development of optical measurement systems for investigating dynamic flow, shape, and surface phenomena.